**Atmospheric
Chemistry
and Physics**

α-pinene photooxidation under controlled chemical conditions – Part 1: Gas-phase composition in low- and high-NOx environments

N. C. Eddingsaas[1], C. L. Loza[1], L. D. Yee[2], J. H. Seinfeld[1,2], and P. O. Wennberg[2,3]

[1]Division of Chemistry and Chemical Engineering, California Institute of Technology, Pasadena, CA, USA
[2]Division of Engineering and Applied Science, California Institute of Technology, Pasadena, CA, USA
[3]Division of Geological and Planetary Sciences, California Institute of Technology, Pasadena, CA, USA

Correspondence to: N. C. Eddingsaas (eddingsa@caltech.edu)

Abstract. The OH oxidation of α-pinene under both low- and high-NOx environments was studied in the Caltech atmospheric chambers. Ozone was kept low to ensure OH was the oxidant. The initial α-pinene concentration was 20–50 ppb to ensure that the dominant peroxy radical pathway under low-NOx conditions is reaction with HO2, produced from reaction of OH with H2O2, and under high-NOx conditions, reactions with NO. Here we present the gas-phase results observed. Under low-NOx conditions the main first generation oxidation products are a number of α-pinene hydroxy hydroperoxides and pinonaldehyde, accounting for over 40 % of the yield. In all, 65–75 % of the carbon can be accounted for in the gas phase; this excludes first-generation products that enter the particle phase. We suggest that pinonaldehyde forms from $RO_2 + HO_2$ through an alkoxy radical channel that regenerates OH, a mechanism typically associated with acyl peroxy radicals, not alkyl peroxy radicals. The OH oxidation and photolysis of α-pinene hydroxy hydroperoxides leads to further production of pinonaldehyde, resulting in total pinonaldehyde yield from low-NOx OH oxidation of ∼33 %. The low-NOx OH oxidation of pinonaldehyde produces a number of carboxylic acids and peroxyacids known to be important secondary organic aerosol components. Under high-NOx conditions, pinonaldehyde was also found to be the major first-generation OH oxidation product. The high-NOx OH oxidation of pinonaldehyde did not produce carboxylic acids and peroxyacids. A number of organonitrates and peroxyacyl nitrates are observed and identified from α-pinene and pinonaldehyde.

1 Introduction

The emissions of biogenic volatile organic compounds (BVOCs) far outnumber those of anthropogenic VOCs (Guenther et al., 1995; Steinbrecher et al., 2009; Monks et al., 2009). Excluding methane, BVOCs are estimated to account for a flux of ∼1150 Tg C yr^{-1}, while anthropogenic VOCs account for only ∼140 Tg C yr^{-1} (Guenther et al., 1995; Goldstein and Galbally, 2007). Important BVOCs include isoprene, (flux of ∼500 Tg C yr^{-1}) and the monoterpenes (∼127 Tg C yr^{-1}) of which α-pinene accounts for ∼50 Tg C yr^{-1} (Guenther et al., 1995; Chung and Seinfeld, 2002). Because they are unsaturated, these compounds are highly reactive towards OH, O_3, and NO_3 and thus play an important role in tropospheric chemistry. The atmospheric oxidation of BVOCs also results in the formation of secondary organic aerosol (SOA). Monoterpenes are significant sources of SOA due to their large emission rate and high SOA yield (Hoffmann et al., 1997; Pye et al., 2010).

The gas-phase oxidation of simple alkanes and alkenes is well understood and most tropospheric chemical mechanisms use laboratory studies of reactions of these species to inform the parameterization of the atmospheric oxidation of VOCs. Many BVOCs, including isoprene, which has a conjugated double bond system, and α-pinene which is a bicyclic hydrocarbon with an endocyclic double bond, however, have much more complicated chemistry than the simple alkanes and alkenes. For example, recent experimental and theoretical studies with isoprene have shown that its atmospheric chemistry is not well modeled by the reactions of simple

Table 1. Experimental conditions.

Date	Hydrocarbon	Concentration (ppb)	OH Source	Aerosol seed[a]	Length of experiment (hours)
5 May 2010	α-pinene	45	H_2O_2	No seed	12
6 May 2010	α-pinene	50	HONO	No seed	10
7 May 2010	α-pinene	48	H_2O_2	AS	11
9 May 2010	α-pinene	52	HONO	AS	8
10 May 2010	α-pinene	47	H_2O_2	AS+SA	11
11 May 2010	α-pinene	46	HONO	AS+SA	10
12 May 2010	α-pinene	20	H_2O_2	No seed	19
13 May 2010	α-pinene	42	CH_3ONO	No seed	8
14 May 2010	α-pinene	47	H_2O_2	AS	12
17 May 2010	α-pinene	48	CH_3ONO	AS	8
18 May 2010	α-pinene	47	H_2O_2	AS+SA	12
19 May 2010	α-pinene	44	CH_3ONO	AS+SA	8
2 June 2010	α-pinene	45	H_2O_2	AS	12
3 June 2010	α-pinene	45	CH_3ONO	AS	8
4 June 2010	Pinonaldehyde	–[b]	H_2O_2	No Seed	9
8 Feb 2011	α-pinene	43	H_2O_2	No seed	8
14 Feb 2011	Pinonaldehyde	–[b]	H_2O_2	No seed	9
16 Feb 2011	α-pinene	31	CH_3ONO	No seed	3
17 Feb 2011	Pinonaldehyde	–[b]	CH_3ONO	No seed	4

[a] AS: ammonium sulfate, AS+SA: ammonium sulfate and sulfuric acid.
[b] The initial concentration of pinonaldehyde was not determined.

alkenes, especially under low-NO_x (NO and NO_2) conditions (Paulot et al., 2009b; Peeters and Muller, 2010; Crounse et al., 2011).

α-pinene is a ten-carbon bicyclic hydrocarbon with an endocyclic double bond and, therefore, has the potential to react in ways not represented by simple alkenes. In addition, α-pinene is highly reactive with both O_3 and OH, reacting in the atmosphere with α-pinene nearly equally, adding to the richness of its atmospheric photochemistry (Capouet et al., 2008). Despite a number of studies of OH oxidation of α-pinene, large uncertainties in the identity and yields of its reaction products remain. For instance, the reported yield of pinonaldehyde from the photooxidation of α-pinene ranges from 28 to 87 % in the presence of NO_x and from 3 to 37 % in the absence of NO_x (Arey et al., 1990; Hatakeyama et al., 1991; Noziere et al., 1999; Jaoui and Kamens, 2001; Wisthaler et al., 2001; Aschmann et al., 2002; Lee et al., 2006). In addition, the molecular structures of major products identified by mass (e.g. 184 and 200 daltons) are subject to debate (Aschmann et al., 2002; Vereecken et al., 2007). The photooxidation product with molecular mass 184 has been assigned to an unsaturated hydroperoxy carbonyl (Vereecken et al., 2007) or a dihydroxy carbonyl (Aschmann et al., 2002). A better understanding of α-pinene gas-phase chemistry will increase the accuracy of α-pinene atmospheric chemistry models and provide insight into atmospheric photooxidation mechanisms in general.

In this study, we isolate the peroxy radical reaction pathways to investigate the photochemistry of α-pinene. We have studied these reactions under low-NO_x conditions similar to those found in the atmosphere, where $RO_2 + HO_2$ is the dominant peroxy radical reaction, and other reactions are suppressed ($RO_2 + RO_2$ and reactions with O_3). We contrast these conditions with results from the gas-phase photooxidation of α-pinene under high-NO_x (with varied amounts of NO_2 to study both $RO_2 + NO$ and $RO_2 + NO_2$). We focus our analysis on low-NO_x rather than high-NO_x chemistry because the low-NO_x chemistry of α-pinene is less well-characterized yet it is more atmospherically-relevant (Pye et al., 2010). In a forthcoming paper, SOA yields and composition formed from the controlled chemical conditions described here will be presented.

2 Experimental

Photooxidation experiments of α-pinene were performed in the Caltech dual 28 m^3 Teflon chambers. Details of the chamber facilities have been described elsewhere (Cocker et al., 2001; Keywood et al., 2004). A few photooxidation experiments were performed in a $\sim$1 m^3 bag enclosed in a small, black walled chamber with UV-lights lining one wall, as described by Crounse et al. (2011). 40 W black lights (Sylvania F40/350BL) with emission peak emission at 352 nm were used in both chambers. The light intensity as a function of wavelength (300–800 nm) was measured using a Licor (LI-1800) spectroradiometer. Prior to each run, the chamber was flushed for a minimum of 24 h with dry purified air. While

being flushed, the chamber was irradiated with the chamber lights for a minimum of six hours. The temperature, relative humidity (RH), and concentrations of O_3, and NO_x (NO and NO_2) were continuously monitored. In all experiments the RH was kept below 10 %. Aerosol size distribution and number concentration were measured continuously by a differential mobility analyzer (DMA, TSI model 3081) coupled to a condensation nucleus counter (TSI model 3760). Information on aerosol measurements can be found in part 2, where aerosol formation, growth, and composition are discussed. Table 1 shows a list of conditions for all experiments used in this study. Experiments ran for 3 to 19 h. No gas phase losses to the chamber walls of either α-pinene prior to light irradiation or oxidation products after lights were extinguished was observed.

Experiments were performed under low- and high-NO_x conditions. Under low-NO_x conditions, photolysis of hydrogen peroxide (H_2O_2) was the OH source, while for the high-NO_x experiments the photolysis of nitrous acid (HONO) or methyl nitrite (CH_3ONO) produced OH. For low-NO_x experiments, 280 μL of 50 wt % H_2O_2 was injected into the chamber resulting in an H_2O_2 concentration ∼4 ppm. The two different OH sources used during the high-NO_x experiments provided the mechanism to vary the NO to NO_2 ratio, with a higher quantity of NO_2 in the CH_3ONO experiments. HONO was prepared daily by dropwise addition of 15 mL of 1 wt % $NaNO_2$ into 30 mL of 10 wt % H_2SO_4 in a glass bulb, and then introduced into the chamber with dry air. This process produces NO and NO_2 as side products, which are also introduced to the chamber. CH_3ONO was synthesized, purified, and stored according to the procedure outlined by Taylor et al. (1980). CH_3ONO was warmed from liquid nitrogen temperatures and vaporized into an evacuated 500 mL glass bulb and introduced into the chamber with an air stream of 5 L min⁻¹. After addition of CH_3ONO, 300–400 ppb of NO was added to the chamber to suppress the formation of O_3. Determination of exact NO and NO_2 concentrations using the commercial NO_x monitor was precluded due to interferences by both HONO and CH_3ONO. At the start of all high-NO_x experiments the total NO_x reading (NO, NO_x, and interference from HONO or CH_3ONO) was 800 ppb and NO concentration throughout the experiments was such that the concentration of O_3 never exceeded 5 ppb.

α-pinene was added to the chamber to achieve a concentration of 20–50 ppb by passing dry air through a bulb containing a known volume of α-pinene. The mixing ratio of α-pinene was monitored by gas chromatography (Agilent 6890N) coupled with a flame ionization detector (GC-FID). The GC-FID was calibrated using a 55 L Teflon bag containing a known concentration of pure α-pinene. Gas phase photooxidation products were monitored using triple-quadrupole chemical ionization mass spectrometry (CIMS) (St. Clair et al., 2010).

Details of the operation of the CIMS can be found in a number of previous reports (Crounse et al., 2006; Paulot et al., 2009a; St. Clair et al., 2010) and therefore only a brief description is presented here. The CIMS was operated in negative ion mode using CF_3O^- as the reagent ion, and in the positive ion mode using H_3O^+ for proton transfer mass spectrometry (PTR-MS). In negative mode, CF_3O^- is sensitive to the detection of polar and acidic compounds by either clustering with the analyte (R) resulting in an ion with a mass-to-charge ratio (m/z) MW+85 ($R \cdot CF_3O^-$) or via fluorine ion transfer resulting in m/z MW+19 ($HF \cdot R_{-H}^-$). The dominant ionization mechanism depends mostly on the acidity of the neutral species; highly acidic species such as nitric acid only form the fluorine transfer ion, while non-acidic species such as methyl hydrogen peroxide form only the cluster ion. This separation aids both in the determination of the structure of a molecule and in the identification of isomers. In negative mode, tandem mass spectrometry (MS/MS) was used to help identify functional groups of an analyte. In brief, a parent ion selected in the first quadrupole is exposed to an elevated pressure of N_2 resulting in collision-induced dissociation (CID) in the second quadrupole, and the resulting fragmentation ions are detected in the third quadrupole. Molecules with different functional groups have been shown to fragment differently by CID and thus the detection of certain fragment ions in quadrupole three can aid in the identification of an analyte. For instance, hydroperoxides form a characteristic fragment at m/z 63 (Paulot et al., 2009b).

Standards are not available for most of the VOCs described here and thus the sensitivity of the CIMS is related to the thermal capture rate and the binding energy of the cluster ($VOC \cdot CF_3O^-$). Details on calculating the sensitivity of the CIMS to a given analyte can be found in previous publications (Paulot et al., 2009a,b).

3 Results and discussion

The goal of this study is to determine the gas-phase reaction products and mechanism of the photooxidation of α-pinene by OH under both low-NO_x and high-NO_x conditions. In both cases, the experiment is designed such that α-pinene only reacts with OH and that a single peroxy radical reaction is dominant. Under ambient conditions, α-pinene reacts at an approximately equal rate with O_3 ($k_{O_3} = 9.0 \times 10^{-17}$ cm³ molecules⁻¹ s⁻¹) and OH ($k_{OH} = 5.3 \times 10^{-11}$ cm³ molecules⁻¹ s⁻¹) (Sander et al., 2006; Atkinson et al., 2006). To isolate the OH chemistry, the formation of O_3 was suppressed.

Under low-NO_x conditions, photolysis of H_2O_2 resulted in steady state OH concentration of ∼2×10^6 cm⁻³ and an HO_2 concentration ∼1×10^{10} cm⁻³. The OH and HO_2 concentrations were determined from a kinetic molecular model of α-pinene OH reaction which is described in detail in Sect. 3.2 and in the Supplement. In brief, OH is produced by the photolysis of H_2O_2 and is primarily consumed by reactions with VOCs in the chamber and with H_2O_2. The reaction of OH
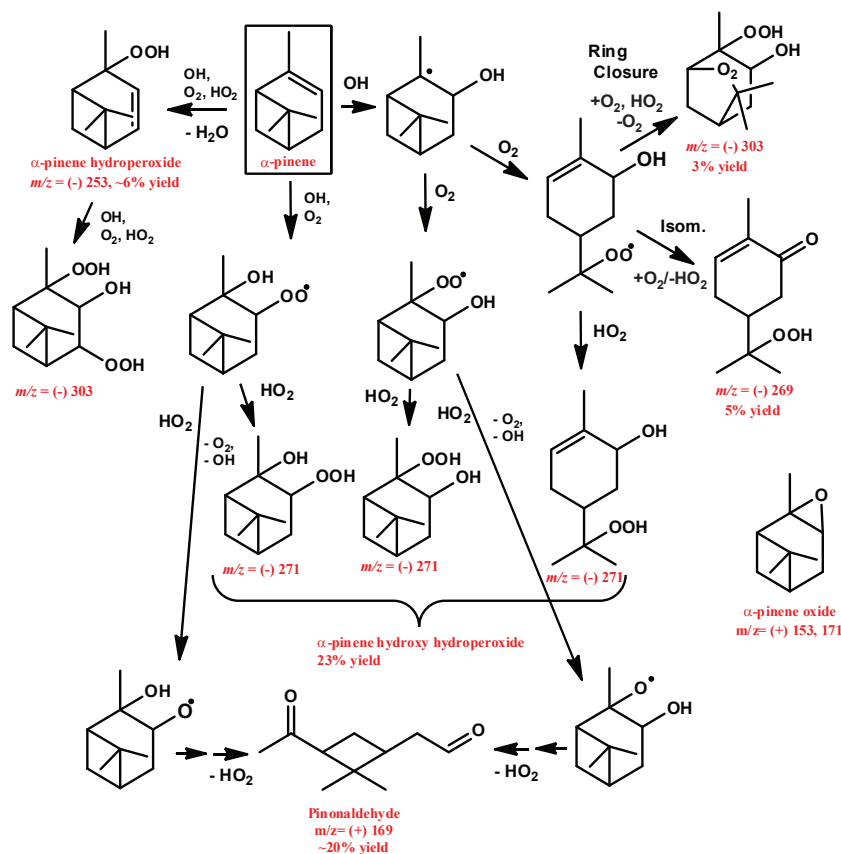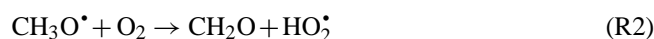
Fig. 1. Pathway of photooxidation of α-pinene under low-NO$_x$ conditions. Species that were observed are labeled in red. The m/z of all species observed in the negative mode are of the complex with CF$_3$O$^-$ (molecular mass + 85). Pinonaldehyde is observed at molecular mass + 1 in the positive mode and α-pinene oxide is observed at molecular mass + 1 and + 19. The observed percent yield for first-generation products is also indicated.
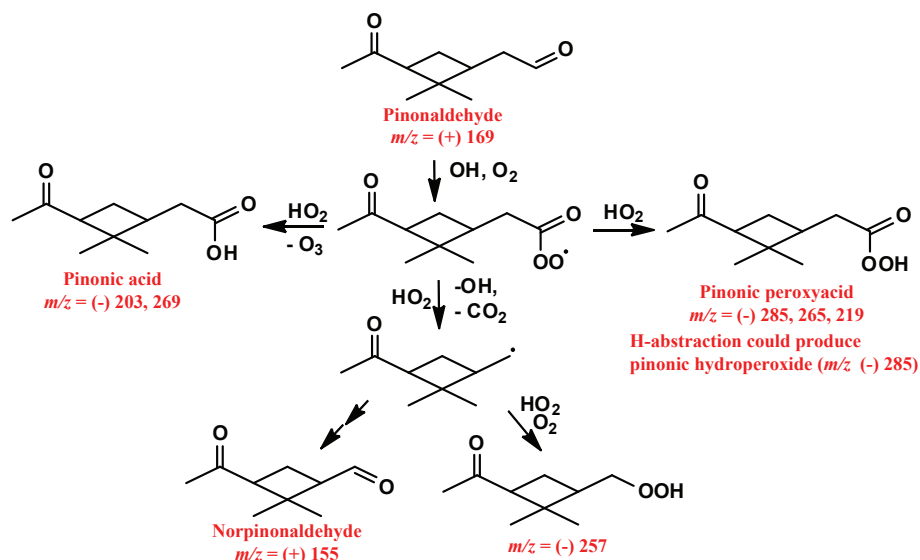
and H$_2$O$_2$ produces HO$_2$. The photolysis rate of H$_2$O$_2$ used in the model and the OH concentration determined by the model were confirmed by comparison of the gas-phase concentrations of H$_2$O$_2$ and α-pinene from the experiment and the model (Fig. S1). These OH concentrations are similar to those observed in the troposphere; however, the HO$_2$ concentrations are about an order of magnitude greater than levels typically observed in rural or remote areas (Lelieveld et al., 2008; Ren et al., 2008; Wolfe et al., 2011). The O$_3$ concentration at the start of each experiment was <4 ppb and typically did not exceed 12 ppb over the course of an experiment (in one experiment, conducted for 20 h, the O$_3$ concentration increased nearly linearly from 4 to 25 ppb). Modeling of these oxidant concentrations indicated that reaction with O$_3$ accounted for <3 % of the α-pinene loss.

In the oxidation of α-pinene by OH, OH adds predominantly to the endocyclic double bond, followed by addition of O$_2$ to the resulting β-hydroxy alkyl radicals producing a number of hydroxy peroxy radicals. OH abstraction of a hydrogen from α-pinene occurs with a yield of ∼12 %, resulting in a peroxy radical when O$_2$ reacts with the alkyl rad-

ical (Capouet et al., 2004). Under low-NO$_x$ conditions the peroxy radicals can react with either HO$_2$ or with another RO$_2$ (self or cross-reactions). Here we seek to emulate atmospheric conditions where RO$_2$ + HO$_2$ dominates. To confirm that the RO$_2$ + HO$_2$ pathway dominated in our experiments, a kinetic model was constructed, as described in Sect. 3.2 and the Supplement. For the experimental conditions (with initial concentration of α-pinene of 20–50 ppb), the kinetic model indicates that less than 1 % of the peroxy radical reactions proceed via RO$_2$ + RO$_2$.

For high-NO$_x$ photooxidation experiments, OH is generated from the photolysis of either HONO or methyl nitrite. When HONO is synthesized, NO and NO$_2$ are produced as side products, which are also introduced to the chamber when HONO is injected. Methyl nitrite is synthesized pure and upon photolysis eventually produces OH and NO$_2$:

$$CH_3ONO + h\nu \rightarrow CH_3O^\bullet + NO \tag{R1}$$

$$CH_3O^\bullet + O_2 \rightarrow CH_2O + HO_2^\bullet \tag{R2}$$

$$HO_2^\bullet + NO \rightarrow OH^\bullet + NO_2 \tag{R3}$$

Fig. 2. Pathway of photooxidation of pinonaldehyde under low-NO_x conditions. Species that were observed are labeled in red. Pinonic acid and pinonic peracid were observed in the negative mode as both the transfer ion (molecular mass + 19) and the complex (molecular mass + 85), pinonic peracid is also observed as the complex minus HF (molecular mass + 65), norpinonaldehyde hydroperoxide was observed as the complex ion, pinonaldehyde and norpinonaldehyde are observed in the positive mode at their molecular mass +1.

When methyl nitrite was used as the OH source, 300 to 400 ppb of NO was added to suppress O_3 production. Under the conditions used, the peroxy radicals formed from the OH reaction of α-pinene react with NO and not RO_2 or HO_2. This is confirmed by the lack of $RO_2 + HO_2$ or $RO_2 + RO_2$ reaction products during high-NO_x photooxidation. The exact ratio of NO to NO_2 is not known as both HONO and methyl nitrite interfere with the signals from the chemiluminescence NO_x instrument; however, it was determined that a higher NO_2 concentration exists during methyl nitrite photolysis due to the increased production of peroxyacyl nitrates (PANs), as detected by CIMS in the negative mode, which result from the $RO_2 + NO_2$ reaction. More details on the detection of, as well as the specific PANs detected will be discussed in Sect. 3.3.

## 3.1 Gas phase composition from low-NO_x photooxidation of α-pinene

The principal first-generation oxidation products observed from the low-NO_x photooxidation of α-pinene were a number of α-pinene hydroxy hydroperoxides and pinonaldehyde. Production of α-pinene hydroperoxide from H-abstraction and α-pinene oxide are also observed (see Fig. 1 for proposed reaction mechanism for α-pinene and Fig. 2 for pinonaldehyde). The time traces from the CIMS are shown in Fig. 3 along with those from a number of the minor oxidation products. The identification of each of these signals is discussed below.

The α-pinene hydroxy hydroperoxides are observed at m/z (−)271 (molecular weight + CF_3O^-) by the CIMS. They

are expected to be a major products of the reaction channel of $RO_2 + HO_2$. Three different α-pinene hydroxy hydroperoxide isomers are formed; two β-hydroxy hydroperoxides and one ring opened hydroxy hydroperoxide containing a double bond (see Fig. 1). The subsequent reaction pathways of these three α-pinene hydroxy hydroperoxides are expected to be different and will lead to distinct reaction products, as discussed in Sect. 3.2. The overall estimated initial yield of the α-pinene hydroxy hydroperoxides is ~23 %. This estimate accounts for the small yield of pinic acid, which has the same molecular weight as these peroxides (MW = 186). Similar to other carboxylic acids, ionization of pinic acid by CF_3O^- yields approximately equal amounts of signal at m/z (−)271 and 205 ($MW_{-H} + HF$). This allows us to use the signal at m/z (−)205 to insure that the pinic acid concentration does not significantly impact the hydroperoxide yield estimate.
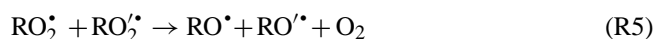
Pinonaldehyde is neither acidic nor is the complex with CF_3O^- significantly strong to be detected in the negative mode and thus is observed only in the positive mode of the CIMS. Pinonaldehyde was synthesized to directly observe its OH oxidation; however, the synthesized sample was not of sufficient purity to calibrate the CIMS response. While we cannot report an absolute yield for pinonaldehyde, we observe that the yield under low-NO_x conditions is 2/3 of that under high-NO_x conditions. As pinonaldehyde is one of the main products of α-pinene oxidation by any atmospheric oxidant, it has been widely studied. Although the reported yield of pinonaldehyde under high-NO_x conditions varies widely from 27–87 % (Arey et al., 1990; Hatakeyama et al., 1991; Noziere et al., 1999; Wisthaler et al., 2001; Jaoui and Kamens, 2001; Aschmann et al., 2002; Lee et al., 2006),
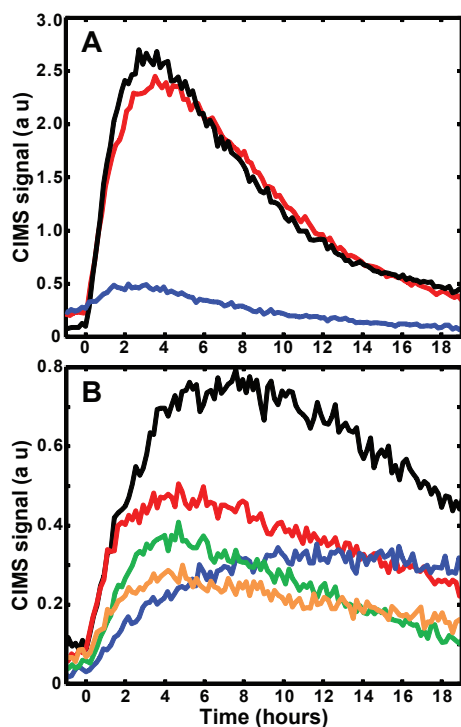
Fig. 3. CIMS time traces of a number of important low-NO$_x$ photooxidation products of α-pinene. **(A)** Main first generation products, m/z $(-)271$ α-pinene hydroxy hydroperoxide (black), m/z $(+)169$ pinonaldehyde (red), m/z $(-)253$ α-pinene hydroperoxide (blue) **(B)** Signals of species that are formed in multiple generations m/z $(-)285$ (black), m/z $(-)269$ (red), m/z $(-)303$ (green), m/z $(-)301$ (orange), and purely second-generation m/z $(-)203$ pinonic acid (blue). The signal from m/z $(+)169$ is the only signal shown from the positive mode and the intensity was divided by 2 for clarity.

most of the measured yields are between 27–35 %. The very high yields were measured by FTIR which may be biased by interference from other carbonyls (Noziere et al., 1999; Hatakeyama et al., 1991). Assuming that under high-NO$_x$ conditions the pinonaldehyde yield is between 27–35 %, we estimate that the low-NO$_x$ yield is about 20 %.

Pinonaldehyde has been observed from the low-NO$_x$ photooxidation of α-pinene previously; however, it is typically assigned as a product of RO$_2$ + RO$_2$ chemistry (Noziere et al., 1999; Larsen et al., 2001). In the present set of experiments, the chemistry is overwhelmingly dominated by RO$_2$ + HO$_2$ (i.e. low α-pinene concentration and relatively high HO$_2$ concentration). This is confirmed by the photooxidation products observed. The two main reaction channels for alkyl peroxy radicals with other RO$_2$ are:

$$RO_2^\bullet + RO_2'^\bullet \rightarrow R{=}O + R'OH + O_2 \tag{R4}$$

$$RO_2^\bullet + RO_2'^\bullet \rightarrow RO^\bullet + RO'^\bullet + O_2 \tag{R5}$$

resulting in the formation of alcohols and carbonyls from Reaction (R4) and alkoxy radicals from Reaction (R5). In the case of α-pinene, these would be β-diols, β-hydroxy carbonyl, and hydroxy alkoxy radicals. The six membered ring of the hydroxy alkoxy radical will then open forming pinonaldehyde. There is no indication of either β-diols or β-hydroxyl carbonyl being formed during the present experiments. In the case of alkyl peroxy radicals reacting with HO$_2$, the main reaction channel is:

$$RO_2^\bullet + HO_2^\bullet \rightarrow ROOH + O_2 \tag{R6}$$
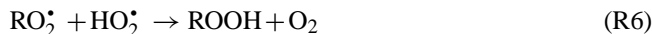
which forms hydroperoxides. For α-pinene, Reaction (R6) will produce the observed α-pinene hydroxy hydroperoxides. For many small alkyl peroxy radicals it has been shown to be the only channel (Hasson et al., 2004; Raventos-Duran et al., 2007; Noell et al., 2010).

If Reaction (R6) was the only channel, there would be no route to pinonaldehyde production. One possible route to pinonaldehyde is a radical channel (see Fig. 1):

$$RO_2^\bullet + HO_2^\bullet \rightarrow RO^\bullet + O_2 + OH^\bullet \tag{R7}$$
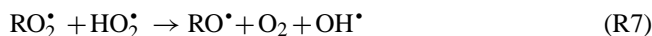
similar to those known to be important for acetyl peroxy radicals (Hasson et al., 2004; Dillon and Crowley, 2008) and possibly for the reaction of OH with toluene (Birdsall et al., 2010). If this is the route to pinonaldehyde formation, an OH recycling channel would also be of importance in the reaction of OH with α-pinene under low-NO$_x$ conditions.

α-pinene hydroperoxide and α-pinene oxide are also observed products of the OH oxidation of α-pinene under low-NO$_x$ conditions. α-pinene hydroperoxide can be formed from H-abstraction by OH, which is estimated to account for about 12 % of the OH reaction with α-pinene (Capouet et al., 2004). Assuming similar CIMS sensitivity to α-pinene hydroperoxide and α-pinene hydroxy hydroperoxide, the yield of α-pinene hydroperoxide is estimated to be $\sim$6 %. The remainder of the H-abstraction branching ratio cannot be accounted for at this time. α-pinene oxide is neither acidic nor is the complex with CF$_3$O$^-$ significantly strong to be detected in the negative mode and thus is observed only in the positive mode at m/z $(+)153$ and 171 as confirmed by direct injection of α-pinene oxide into the chamber. Further evidence of α-pinene oxide formation is presented in part 2 of this series of paper where SOA composition is discussed. α-pinene oxide appears to be a minor product, and the mechanism for its formation by OH oxidation is not known. The mechanism for the formation from O$_3$ oxidation is known and yields of a few percent have been reported (Alvarado et al., 1998; Berndt et al., 2003); however, in the present experiments O$_3$ accounts for less than 3 % of the oxidation of α-pinene.

The oxidation products of pinonaldehyde have been shown to be important in the formation of SOA from the photooxidation of α-pinene. Specifically, pinonic acid, 10-hydroxypinonic acid, and pinic acid have been observed in ambient SOA samples (Kavouras et al., 1998, 1999; Yu

et al., 1999; Laaksonen et al., 2008; Zhang et al., 2010) and in laboratory studies of α-pinene photooxidation (Larsen et al., 2001; Jaoui and Kamens, 2001; Librando and Tringali, 2005). The low-NO$_x$ photooxidation of pinonaldehyde was carried out to determine the contribution of pinonaldehyde oxidation products to the gas and particle phases of α-pinene photooxidation.

Photooxidation of pinonaldehyde accounts for a number of the products observed from α-pinene photooxidation. OH oxidation of pinonaldehyde occurs by H-abstraction, typically from the aldehydic group (59–86 %) (Kwok and Atkinson, 1995; Vereecken and Peeters, 2002) forming an acyl peroxy radical after the addition of O$_2$. The reaction of HO$_2$ with an acyl peroxy radical produces carboxylic acids, peroxyacids, and acetoxy radicals that will decompose to produce CO$_2$ and an alkyl radical. Hasson et al. (2004) have shown that these three pathways occur in roughly equal yields. The reaction pathways and products from pinonaldehyde are shown in Fig. 2. Pinonic acid is observed by the CIMS mostly by its transfer product ion (ratio of m/z $(-)203$ to m/z $(-)269$ is ~9:1), typical of acidic species, while the peroxyacid is observed more by its complex ion (ratio of m/z $(-)219$ to m/z $(-)285$ is ~1:4) (Fig. 4). In addition, we have observed, using synthesized peracetic acid, that peroxyacids are also observed in the negative mode as its molecular mass +65 (complex with CF$_3$O$^-$ − HF) at 10–20 % that of the complex ion (+85). A signal at m/z $(-)265$, ~10 % the intensity of m/z $(-)285$, has been assigned to pinonic peroxyacid providing further evidence of its formation. These two products are formed in roughly equal yields. H-abstraction at carbons other than the aldehydic carbon could also form pinonaldehyde hydroperoxide which would also be detected at m/z $(-)285$, as would 10-hydroxy pinonic acid (product found in SOA). A signal at m/z $(-)257$ that has nine carbons was observed and has been assigned to the hydroperoxide formed from the alkyl radical formed from the decomposition of the acetoxy radical. The formation of norpinaldehyde was also detected. Pinic acid was observed in equal amounts at m/z $(-)205$ and m/z $(-)271$, but is a minor product.

Low-NO$_x$ photooxidation of α-pinene also leads to the pinonaldehyde oxidation products (Fig. 4). Ions at m/z $(-)203$ and $(-)219$ assigned to the transfer ions of pinonic acid and pinonic peroxyacid are observed to be second generation products from α-pinene photooxidation, as would be expected arising from the oxidation of pinonaldehyde. The ion at m/z $(-)257$ assigned to the C$_9$ hydroperoxide produced from pinonaldehyde photooxidation is also observed to be second generation. Pinonic acid and pinonic peroxyacid are also observed as the complex ion at m/z $(-)269$ and $(-)285$ respectively. The time traces for m/z $(-)269$ and m/z $(-)285$ from the photooxidation of α-pinene are not purely from first or second generation products (see Figs. 3 and 4) but a combination of the two. The second generation products observed as these two ions are pinonic acid and pinonic peroxyacid, evident from their transfer ions, while
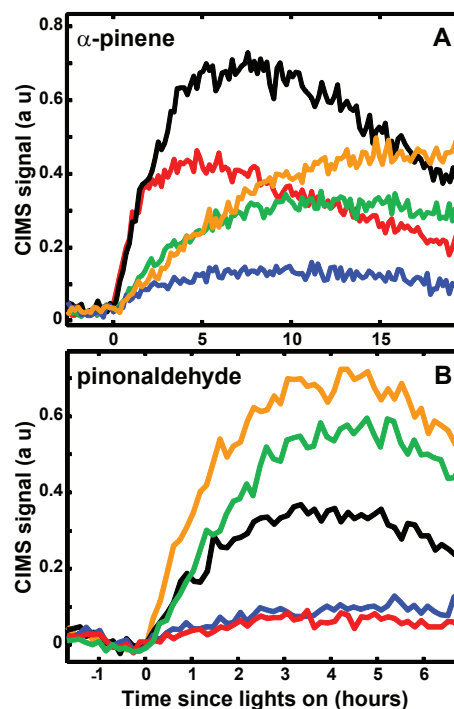
Fig. 4. Comparison of CIMS signals from low−NO$_x$ photooxidation of **(A)** α-pinene and **(B)** pinonaldehyde; m/z $(-)285$ (black), m/z $(-)269$ (red), m/z $(-)257$ (orange), m/z $(-)219$ (blue), and m/z $(-)203$ (green). Pinonaldehyde photooxidation produces pinonic peroxyacid observed at both m/z $(-)285$ and $(-)219$, pinonic acid observed at both m/z $(-)269$ and $(-)203$, and a C$_9$ hydroperoxide observed at m/z $(-)257$. The pinonaldehyde photooxidation products are observed from α-pinene photooxidation along with additional first-generation signals at m/z $(-)269$ and $(-)285$ from first-generation photooxidation products.

the first generation products arise from the photooxidation of α-pinene. Oxidation products of these molecular mass (184 and 200) have been observed and theoretically proposed from the photooxidation of α-pinene in the presence of NO (Aschmann et al., 2002; Vereecken et al., 2007). Under high-NO$_x$ conditions, Aschmann et al. (2002) observed molecules at these masses and assigned them to a dihydroxy carbonyl and a trihydroxy carbonyl that would be formed by a number of isomerization steps as well as multiple reactions of peroxy radicals with NO to form alkoxy radicals. Vereecken et al. (2007) indicate that molecules with these molecular weights could be formed by isomerization reactions after ring opening, while the molecule with MW = 200 is produced from a reaction of NO with the peroxy radical. In both mechanisms, alkoxy radicals are essential. Alkoxy radicals appear to form from the reaction of the initially formed α-pinene hydroxy peroxy radical intermediates with HO$_2$, and this is a possible route; however, at this point, the structure of these molecules is unknown. These are, however, clearly polyoxygenated species formed from the primary oxidation

of α-pinene and their most likely molecular formulas are $C_{10}H_{16}O_3$ and $C_{10}H_{16}O_4$.

Highly oxidized species at m/z $(-)301$ and $(-)303$ are also observed as first generation products (see Fig. 3). Both signals decay similarly to the signals at m/z $(-)269$ and $(-)285$, indicating that they are also formed as later generation products. The most likely structure for the first-generation species at m/z $(-)303$ is an α-pinene hydroxy hydroperoxide with a bridging peroxy group that results from the ring closing channel of the ring opened hydroxy hydroperoxide as shown in Fig. 1. This mechanism has been postulated by Vereecken et al. (2007). The addition of one hydroxyl group and two hydroperoxyl groups decreases the vapor pressure about eight orders of magnitude making this product a likely aerosol phase component (Capouet and Müller, 2006). The photooxidation of α-pinene hydroperoxide will produce a hydroxy dihydroperoxide that will also be observed at m/z $(-)303$ thus accounting for the slow decay of the signal. We do not know the structure of the photooxidation product(s) at m/z $(-)301$. Given the molecular weight, the structure potentially includes one carbonyl and two hydroperoxyl groups. Whatever the structure, the vapor pressure will be greatly reduced from that of α-pinene, once again making it a potential SOA component.

Another route to the formation of the low vapor pressure oxidation products at m/z $(-)301$ and $(-)303$ is peroxy radical isomerization. Peroxy radical isomerization has recently been extensively studied for the isoprene system both theoretically (Peeters et al., 2009; da Silva et al., 2010; Nguyen et al., 2010) as well as experimentally (Crounse et al., 2011). It has been shown that peroxy radical isomerization most often occurs via a six or seven membered intermediate (Perrin et al., 1998; Blin-Simiand et al., 2001; Jorand et al., 2003). When OH adds to the tertiary carbon of the double bond the peroxy radical on the secondary carbon can form a seven membered ring with the hydrogen of either the secondary carbon in the four membered ring or one of primary carbons attached to the four membered ring. After isomerization, reaction with O_2 and HO_2 will result in the formation of α-pinene hydroxy dihydroperoxide which would be detected at m/z $(-)303$. See Fig. S2 in the Supplement for proposed mechanism. When OH adds to the secondary carbon of the double bond, a seven membered intermediate can form with the other tertiary carbon of the four membered ring ultimetly forming α-pinene hydroxy dihydroperoxide. Similarly, the α-pinene hydroxy hydroperoxide peroxy radical formed from isomerization from the addition of OH to the secondary carbon can form a six membered ring with the hydrogen on the carbon α to the hydroxyl group. This isomerization would result in the formation of α-pinene carbonyl dihydroperoxide which would be observed at m/z $(-)301$. For the species observed at m/z $(-)301$ and $(-)303$ to be formed via isomerization, the rate of peroxy radical isomerization would have to be competitive with that of $RO_2 + HO_2$. In the present experiments $[HO_2]$ is $\sim 1 \times 10^{10}$ molecules cm^{-3} so

the rate of loss of α-pinene hydroxy peroxy radical by reaction with HO_2 is $\sim 0.2\,s^{-1}$. In the atmosphere the HO_2 concentration is about an order of magnitude less, so for isomerization to be competitive (10 % of peroxy radical reaction) the rate would have to be $\sim 0.002\,s^{-1}$. In the isoprene system the isomerization rate has been found to be $0.002\,s^{-1}$ with conformer specific rates being much faster (Crounse et al., 2011). At this time there have been no experimental studies on the isomerization rate in the α-pinene system so it is unknown what the rate is and therefor its atmospheric relevance. If the rate of isomerization is competitive with reaction with HO_2 in the atmosphere, more low vapor pressure species capable of partitioning into the aerosol will be formed than were observed in this study.

3.2 Kinetic model of low-NO$_x$ photooxidation of α-pinene

To gain a better understanding of the low-NO$_x$ photooxidation of α-pinene, a kinetic model was assembled and compared to the time traces of α-pinene and the reaction products measured during the photooxidation of 19.8 ppb α-pinene and 4 ppm H_2O_2. The kinetic model was constructed using Kintecus modeling software (Ianni, 2002). When available, rate constants from literature were used; however, a majority of the rate constants are not known. In these cases, reaction rates with respect to OH oxidation were estimated using the structural activity relationship derived by Kwok and Atkinson (Kwok and Atkinson, 1995). This method has been shown to predict rate constants to within a factor of two for most species (see Tables S1 and S2 for lists of photooxidation products, reactions, and reaction rates used in this model). The rate constants were then modified slightly to best fit the data. The rate constants for $RO_2 + HO_2$ and $RO_2 + RO_2$ were taken from the estimates used for the Master Chemical Mechanism (Saunders et al., 2003). Photolysis was included for hydrogen peroxide, the organic hydroperoxides, and for pinonaldehyde. The photodissociation frequencies (j) were determined from the spectral radiance measured from the chamber lights and the absorption cross sections reported in the literature for hydrogen peroxide and pinonaldehyde and estimated for the organic hydroperoxides from reported cross sections of similar hydroperoxides (Atkinson et al., 2006; Sander et al., 2006).

For the model to be accurate, the concentration of OH and HO_2 need to be correct. OH is produced from photolysis of H_2O_2 which initially reacts with hydrocarbons in the chamber as well as H_2O_2. It is the reaction of OH with H_2O_2 that produces HO_2. The value of $j_{H_2O_2}$ was confirmed by comparing the simulated loss of H_2O_2 (photolysis and reaction with OH) to the time trace observed from the CIMS (see SI Fig. S1). The comparison of the simulated loss of α-pinene, using the recommended rate constant for the reaction of α-pinene with OH from the IUPAC database (Atkinson et al., 2006), with the the observed loss of α-pinene also confirms
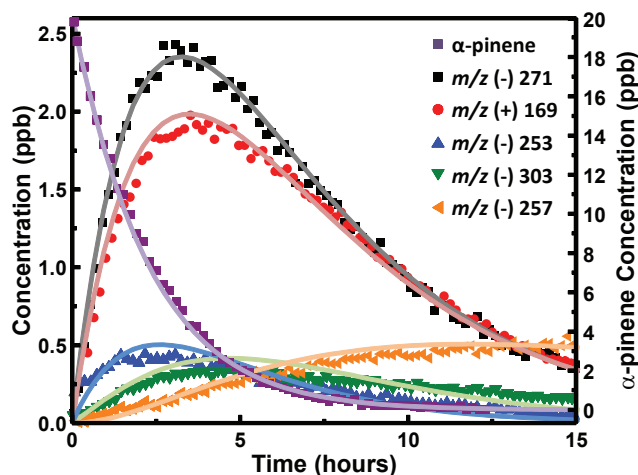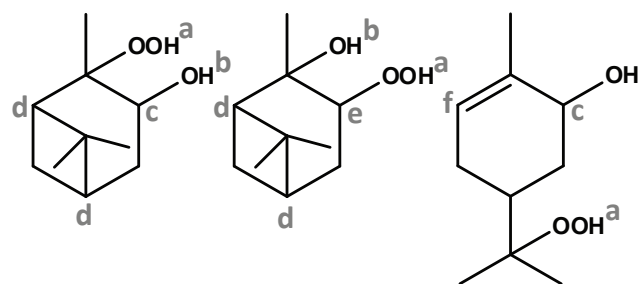
Fig. 5. Time-dependent observed (points) versus simulated (lines) concentrations from the photooxidation of 19.8 ppb of α-pinene. Represented are α-pinene (purple), α-pinene hydroxy hydroperoxide (black), pinonaldehyde (red), α-pinene hydroperoxide (blue), α-pinene hydroxy dihydroperoxide (green), and the C_9 hydroperoxide from pinonaldehyde (orange). See the Supplement for structural information and kinetic model.

Fig. 6. Structure of the hydroxy hydroperxides formed from the low-NO_x photooxidation of α-pinene, the most likely positions for reaction with OH are also shown; H-abstraction **(a–e)** and OH addition **(f)**.

the simulation produces the correct amount of OH (see Fig. S1 in the Supplement). The modeled OH concentration quickly reaches 2.2×10^6 molecules cm^{-3} and is approximately constant between 2.2–2.5×10^6 molecules cm^{-3} over the course of the experiment, while the HO_2 concentration rapidly plateaus at about 1×10^{10} molecules cm^{-3}. In addition, the rate constant of OH with pinonaldehyde was confirmed from the experiment where pinonaldehyde was directly injected into the chamber. Pinonaldehyde is lost by reaction with OH as well as photolysis ($\sim$10 % of overall reaction), and the best fit to the data is achieved with $k_{\text{pinonaldehyde+OH}} = 3.7 \times 10^{-11}$ cm^3 molecules^{-1} s^{-1} (Fig. S3 in the Supplement). This rate constant is within the error recommended by the IUPAC database and the latest measurement of this reaction rate by Davis et al. (2007); Atkinson et al. (2006).

Figure 5 shows the time traces of α-pinene and several of the photooxidation products along with the simulated concentrations from the kinetic model. The oxidation products in Fig. 5 are representative of first-generation products (α-pinene hydroxy-hydroperoxides, pinonaldehyde, and α-pinene hydroperoxide) and a second-generation product (C_9 hydroperoxide from pinonaldehyde) (see Table S1 for structural information of each compound). The one exception is the highly oxygenated compound observed at m/z (−)303 (assigned to hydroxyl dihydroperoxide) that is both a first- and second-generation product, and due to its high degree of oxidation and low volatility is predicted to partition into the particle phase. As noted in Sect. 3.1, pinic acid is a minor second generation product that is observed at m/z (−)205 and m/z (−)271 in roughly equal amounts. This small yield was

accounted for in determining the concentration of α-pinene hydroxy hydroperoxides. Using the fastest $RO_2 + RO_2$ rate constant for α-pinene hydroxy peroxy radicals from MCM, only 0.05 % of the peroxy radical is predicted to react through the $RO_2 + RO_2$ channel. Including all of the identified first-generation products (these presented here along with the products at m/z (−)269, 285, and 301), 65–75 % of the carbon can be accounted for, and this does not include compounds that are expected to partition into the aerosol phase.

Pinonaldehyde, in the present set of experiments, is formed from the $RO_2 + HO_2$ reaction channel of two of the α-pinene hydroxy peroxy radicals, and the reaction rate with OH has been well characterized. However, based on these formation and loss mechanisms for pinonaldehyde, the simulated pinonaldehyde decays far too quickly; therefore, pinonaldehyde must also be produced as a second-generation oxidation product. Of the first-generation products, the most likely candidates to produce pinonaldehyde from a reaction with OH are the α-pinene hydroxy hydroperoxides.

There are a number of paths by which the α-pinene hydroxy hydroperoxides will form pinonaldehyde. First of all, the hydroperoxide will not only react with OH but will also undergo photolysis. Photolysis cleaves the weak O-O bond of the hydroperoxide producing an alkoxy radical that will produce pinonaldehyde. We estimate, however, that photolysis represents $\sim$3 % of the α-pinene hydroxy hydroperxide loss and thus does not provide mass closure between the data and the simulation.

Figure 6 shows the three hydroxy hydroperoxides that are formed from low-NO_x photooxidation of α-pinene, two β-hydroxy hydroperoxides and a ring-opened one that includes a double bond. The β-hydroxy hydroperoxides have a number of places where OH hydrogen abstraction could occur (Fig. 6), the carbon α to the alcohol; carbon α to the hydroperoxyl group; either of the tertiary carbons; the alcoholic hydrogen; or the hydroperoxy hydrogen. Hydrogen abstraction from an alcohol will mostly occur from the α carbon which has been shown to result in the formation of a

carbonyl and HO$_2$ (Carter et al., 1979; Atkinson, 1986; Grosjean, 1997). Presumably this would form a hydroperoxy carbonyl, a mass analog of the known second-generation product pinonic acid. As there are first- and second-generation products with m/z ($-$)269, it is not clear how important this H-abstraction channel is. There have only been a few hydroperoxides whose H-abstraction reaction rates and product distributions have been studied: methyl, ethyl and tert-butyl (Vaghjiani and Ravishankara, 1989; Niki et al., 1983; Wang and Chen, 2008; Baasandorj et al., 2010). It has been shown that the OO-H bond is fairly labile and H-abstraction from both the hydroperoxide as well as the α-carbon will occur. H-abstraction from the hydroperoxyl group will result in reformation of the peroxy radical with the same branching ratio of products from the initial reaction forming, among other species, pinonaldehyde and hydroxy hydroperoxide. H-abstraction from the α-carbon of the hydroperoxy group would presumably form a hydroxy carbonyl, which is a mass analog of α-pinene hydroperoxide. In the model, the signal associated with α-pinene hydroperoxide is fit well with a production channel from α-pinene and a reaction rate with OH that is nearly as fast as α-pinene itself, suggesting that it is unlikely that there is a second-generation product formed at this mass. It is possible that following hydrogen abstraction, the ring is cleaved, ultimately resulting in the formation of pinonaldehyde. Finally, H-abstraction from either of the tertiary carbons will produce more highly oxygenated species, including a hydroxyl dihydroperoxide (m/z ($-$)303). Of these different H-abstraction pathways, those involving the hydroperoxide and carbons α to the hydroperoxy and hydroxyl groups are expected to dominate. The ring opened hydroxy hydroperoxide has a highly reactive double bond instead of one of the tertiary carbons. After addition of OH to the double bond, the reaction will most likely proceed in one the following ways: formation of a dihydroxy dihydroperoxide or intermolecular reaction of the alkyl radical with the hydroperoxy group forming a ring with one oxygen and releasing OH. The former product has not been observed in the present experiments; however, this highly oxidized compound has a low vapor pressure and is expected to primarily reside in the particle phase. The later product is a mass analog of the hydroxy hydroperoxide, and the two species are indistinguishable by CIMS.

In the simulation, all the pathways for reaction of the α-pinene hydroxy hydroperoxides were considered and the contribution of each was varied until the simulation best fit the data based on a least-squares analysis of α-pinene hydroxy hydroperoxide and pinonaldehyde. The best fit results when 58 % of the reaction produces pinonaldehyde directly while another 25 % reforms the peroxy radical, resulting in a net ~33 % of α-pinene producing pinonaldehyde from low-NO$_x$ photooxidation. This is important since the oxidation products of pinonaldehyde are main SOA components. There is need for further studies on the photooxidation of α-pinene hydroxy hydroperoxides to confirm these reaction pathways

and branching ratios; however, the data and kinetic model strongly indicate that pinonaldehyde is produced from the OH oxidation of α-pinene hydroxy hydroperoxides under low-NO$_x$ conditions.

3.3 Gas-phase composition from high-NO$_x$ photooxidation of α-pinene

Figure 7 shows the proposed reaction mechanism of α-pinene photooxidation under high-NO$_x$ conditions. This mechanism and the following discussion of the reaction products are not intended to be all-inclusive. The photooxidation of α-pinene under high-NO$_x$ conditions produces a large variety of compounds through functionalization and fragmentation reactions. We observe signals at many masses but, for brevity, we only focus on those of the major products of α-pinene and pinonaldehyde high-NO$_x$ OH oxidation.

In the presence of NO$_x$, the main photooxidation products of α-pinene are pinonaldehyde, organonitrates, and isomerization products from the alkoxy radical formed from the reaction of NO with the peroxy radical. The yield of pinonaldehyde is 1.5 times that formed in the absence of NO$_x$, and, as mentioned above, previous studies show that it is 27–35 %. Capouet et al. (2004) estimates α-pinene hydroxy nitrate yield to be ~15 %. Alkoxy radical isomerization products are observed at m/z ($-$)269 (MW 184) and m/z ($-$)285 (MW 200). These isomerization products have been observed previously and have been assigned to either a dihydroxy carbonyl and a trihydroxy carbonyl (Aschmann et al., 2002) or to ring opened substituted hydroperoxides (Vereecken et al., 2007). In the present study, the yield of the isomerization products was found to be less than 20 %. The OH addition to the double bond can also result in prompt ring opening of the four-membered ring. Further reactions of the ring-opened alkyl radical will result in fragmentation producing an alkyl radical and acetone (see Fig. 7). This is a minor pathway, as the total acetone yield observed was less than 10 %, including the production of acetone from the photooxidation of pinonaldehyde. Finally, there is a first-generation species observed at m/z ($-$)301, which was also present during low-NO$_x$ photooxidation. A likely molecular formula is C$_{10}$H$_{16}$O$_5$, but the identity of this molecule is unknown. The same oxidation products were observed from high-NO$_x$ photooxidation, regardless of OH source, HONO or methyl nitrite.

The photooxidation of pinonaldehyde was studied using methyl nitrite as the OH source. Figure 8 shows the proposed mechanism and products of this reaction. There have been two theoretical studies on the H-abstraction of pinonaldehyde (Kwok and Atkinson, 1995; Vereecken and Peeters, 2002). Kwok and Atkinson (1995) indicate that 86 % of the abstraction will occur at the aldehydic hydrogen, while Vereecken and Peeters (2002) determined that 59 % will be of the aldehydic hydrogen, 23 % from the carbon β to the aldehydic carbon, and 14 % from the tertiary carbons. The
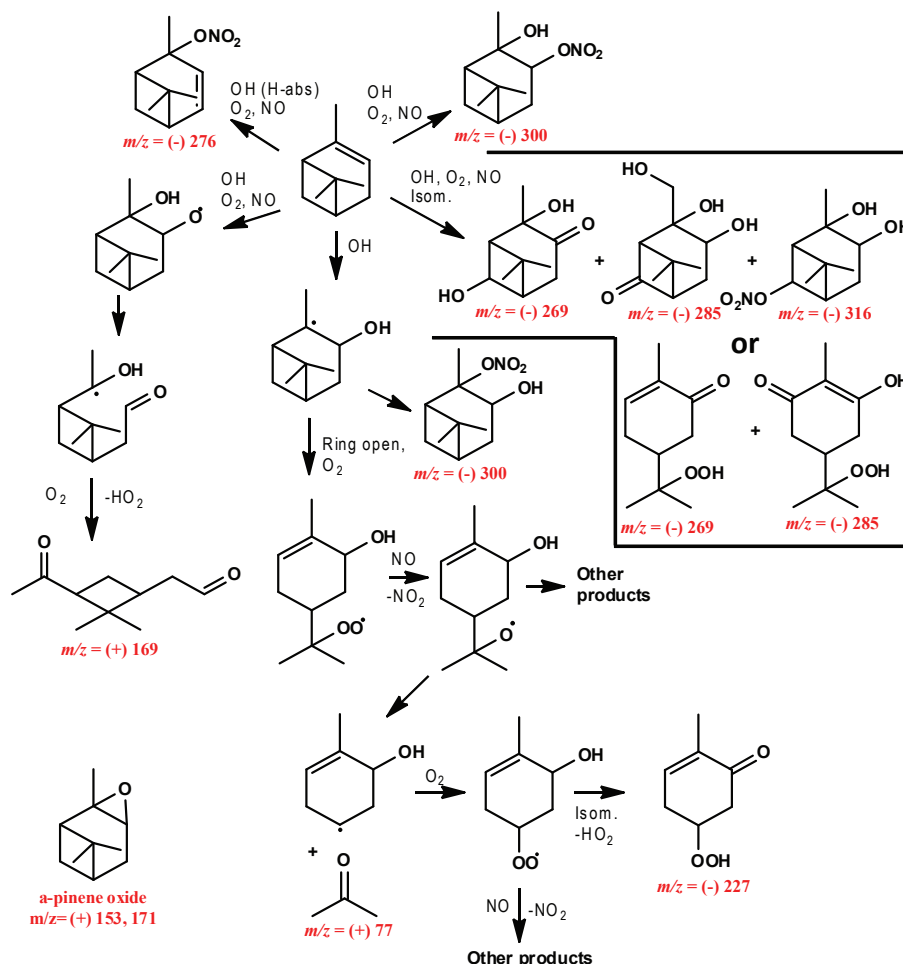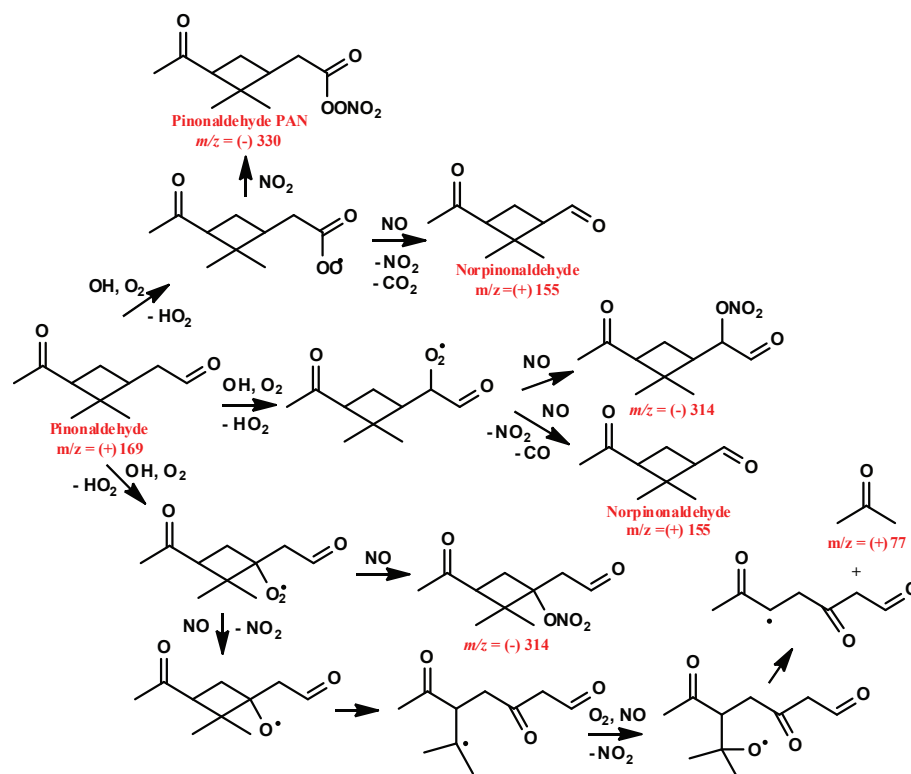
Fig. 7. Pathways of photooxidation of α-pinene under high-NO$_x$ conditions, the structures for m/z (−)269 and (−)285 (MW 184 and 200) are those proposed by Aschmann et al. (2002) and Vereecken et al. (2007). Ion of compounds detected by CIMS are indicated in red.

products expected, and observed, of the primary channel (H-abstraction of the aldehydic hydrogen) are pinonaldehyde PAN, formed from reaction of the acyl peroxy radical with NO$_2$ or norpinonaldehyde, formed from reaction of the acyl peroxy radical with NO (see Fig. 8 for structures and mechanisms). H-abstraction from the carbon β to the aldehydic carbon produces either pinonaldehyde nitrate or norpinonaldehyde with the loss of CO. Finally, H-abstraction from the tertiary carbons produces pinonaldehyde nitrate or a tertiary alkoxy radical. One potential reaction pathway for the tertiary alkoxy radical is the decomposition to form acetone (see Fig. 8), which is observed in low yield from high-NO$_x$ photooxidation of pinonaldehyde. Once formed, norpinonaldehyde will be oxidized in similar fashion to pinonaldehyde. The signal for pinonaldehyde PAN is 4–8 times that of pinonaldehyde nitrate (from all high-NO$_x$ experiments, α-pinene and pinonaldehyde) depending on the NO$_2$ concentration relative to NO. The observed signal of the norpinonaldehyde PAN to norpinonaldehyde nitrate from the photooxidation of pinonaldehyde was greater than 14 to 1. Pinonaldehyde PAN

is formed from an acyl peroxy radical while pinonaldehyde nitrate will be formed from an alkyl peroxy radical. The formation of an acyl peroxy radical is favored over the formation of an alkyl peroxy radical from H-abstraction of pinonaldehyde and thus the formation of pinonaldehyde PANs is expected to be formed in higher yield than pinonaldehyde nitrate. A quantitative yield of the PAN is not known because the CIMS has not been calibrated for these compounds. The product distribution from the photooxidation of pinonaldehyde indicates that it does not add much to the total organonitrate yield from the photooxidation of α-pinene. Pinonic acid and pinic acid were not observed in the gas phase from either α-pinene or pinonaldehyde photooxidation under high-NO$_x$ conditions.

An array of organonitrates and PANs are observed from the photooxidation of α-pinene. In addition to those previously discussed, nitrates were observed at m/z (−)276, 316, 318, 320, and 332 as well as PANs at m/z (−)346 and (−)362 (most likely observed as the molecular complex ion MW + 85). The unidentified organonitrates and PANs are

Fig. 8. Pathways of photooxidation of pinonaldehyde under high-NO$_x$ conditions, H-abstraction by OH occurs predominantly at the aldehydic carbon. Ion of compounds detected by CIMS are indicated in red.

formed in much lower yields than those identified earlier. Nitrates and PANs are distinguished from each other by the nature of their decay. PANs thermally decompose so their gas-phase concentration will continue to decrease even after OH is no longer present. Norpinonaldehyde PAN is observed at m/z ($-$)316; however, comparing the time traces of this ion from pinonaldehyde photooxidation and α-pinene photooxidation, there appears to be a product formed from α-pinene as well. This could be the α-pinene dihydroxynitrate proposed by Aschmann et al. (2002). One interesting observation is that α-pinene hydroxy nitrate is lost from the gas phase at nearly an equal rate as pinonaldehyde. This is in contrast to the other organonitrates, whose signals are stable once they are formed.

The products of high-NO$_x$ photooxidation of α-pinene are the same regardless of NO$_2$ level; however, there are a few differences in concentrations of certain species depending on the level of NO$_2$. The most noticeable difference in the gas-phase composition depending on the [NO$_2$] is the concentration of PANs, which are greater at high NO$_2$ (methyl nitrite photolysis). This is expected as the NO$_2$ concentration is higher in the methyl nitrite experiments resulting in a greater likelihood of NO$_2$ reacting with the acyl peroxy radicals produced from pinonaldehyde and norpinonaldehyde. The concentrations of isomerization products at m/z ($-$)269 and ($-$)285 showed a dependence on seed particle acidity when

HONO was used as the OH source but not when CH$_3$ONO was used as the OH source. In the case of the HONO source, the isomerization products were observed to be lower in the presence of an acidic seed. A discussion of why the products observed at m/z ($-$)269 and ($-$)285 are dependent on aerosol acidity only for the HONO case will be presented in part 2. The only other observed difference in the gas phase was the concentration of nitric acid, which was 1.5 times greater when methyl nitrite was the OH source then when HONO was the OH source.

4   Atmospheric implications

Under low-NO$_x$ photooxidation of α-pinene, pinonaldehyde is produced by RO$_2$ + HO$_2$ chemistry in high yields. RO$_2$ + RO$_2$ chemistry is not the source, as is commonly assumed. While the atmospheric concentrations of HO$_2$ and RO$_2$ are similar, the rate constant of RO$_2$ + HO$_2$ is typically 1–4 orders of magnitude greater than RO$_2$ + RO$_2$. The further OH oxidation of pinonaldehyde produces a number of low volatility carboxylic acids and peroxyacids, which are important SOA components. While the only product with higher yield than pinonaldehyde is α-pinene hydroxy hydroperoxide, pinonaldehyde is also produced from the photolysis and OH oxidation of α-pinene hydroxy hydroperoxide. Including

the reaction channels of α-pinene hydroxy hydroperoxide that form pinonaldehyde (58 %) and assuming 19 % direct yield from α-pinene, the overall oxidation of α-pinene by OH under low-NO_x conditions has a pinonaldehyde yield of ~33 % .

Pinonic acid is an important tracer for SOA formed from α-pinene oxidation and is believed to be the precursor for other SOA tracers, such as 3-methyl-1,2,3-butanetricarboxylic acid (Szmigielski et al., 2007; Müller et al., 2012). Pinonic acid is not observed from the high-NO_x photooxidation of α-pinene, which is not surprising since there is no clear formation mechanism for it in the gas phase. Thus, observation of pinonic acid and the tracers derived from pinonic acid likely point to either low-NO_x oxidation of α-pinene by OH or ozonolysis under high-NO_x conditions. The aerosol-phase composition of these carboxylic acids as well as other carboxylic acids from α-pinene photooxidation will be discussed in detail in Part 2.

The gas-phase chemistry of α-pinene and its photooxidation products is complex and not well represented by the reactions of simple alkenes. By isolating the critical peroxy radical reactions, the products and branching ratios of a number of key reactions have been better constrained. Perhaps most importantly, we suggest that the formation of pinonaldehyde from low-NO_x photooxidation of α-pinene via $RO_2 + HO_2$ proceeds by the formation of an alkoxy radical and OH recycling. This reaction scheme has previously been shown to be important only for acyl peroxy radicals and possibly toluene. Unfortunately, the nature of the potential energy surface leading to radical recycling in the reactions of HO_2 with peroxy radicals has not been fully formulated. Is the OH recycling channel available due to the β hydroxyl group withdrawing electron density from the peroxy group, the bicyclic ring structure of α-pinene, or some other reason all together? To date, most of the detailed work on the reaction of alkyl peroxy radicals with HO_2 has focused on small, unsubstituted peroxy radicals; further work on a broader set of peroxy radicals, including atmospherically relevant VOCs such as monoterpenes and sesquiterpenes, is clearly needed to elucidate the physical chemistry. Finally, we suggest that there is a large secondary pinonaldehyde source from the photooxidation and/or photolysis of the three pinene hydroxy hydroperoxides produced from α-pinene.

Supplementary material related to this article is available online at: http://www.atmos-chem-phys.net/12/6489/2012/acp-12-6489-2012-supplement.pdf.

References

Alvarado, A., Tuazon, E. C., Aschmann, S. M., Atkinson, R., and Arey, J.: Products of the gas-phase reactions of O(^{3}P) atoms and O_3 with alpha -pinene and 1,2-dimethyl-1-cyclohexene, J. Geophys. Res.-Atmos., 103, 25541–25551, doi:10.1029/98JD00524, 1998.

Arey, J., Atkinson, R., and Aschmann, S. M.: Produt study of the gas-phase reactions of monoterpenes with the OH radical in the presence of NO_x, J. Geophys. Res., 95, 18539–18546, doi:10.1029/JD095iD11p18539, 1990.

Aschmann, S. M., Atkinson, R., and Arey, J.: Products of reaction of OH radicals with alpha-pinene, J. Geophys. Res.-Atmos., 107, D14, doi:10.1029/2001JD001098, 2002.

Atkinson, R.: Kinetics and mechanisms of the gas-phase reactions of the hydroxyl radical with organic compounds under atmospheric conditions, Chem. Rev., 86, 69–201, 1986.

Atkinson, R., Baulch, D. L., Cox, R. A., Crowley, J. N., Hampson, R. F., Hynes, R. G., Jenkin, M. E., Rossi, M. J., Troe, J., and IUPAC Subcommittee: Evaluated kinetic and photochemical data for atmospheric chemistry: Volume II – gas phase reactions of organic species, Atmos. Chem. Phys., 6, 3625–4055, doi:10.5194/acp-6-3625-2006, 2006.

Baasandorj, M., Papanastasiou, D. K., Talukdar, R. K., Hasson, A. S., and Burkholder, J. B.: $(CH_3)_3$COOH (tert-butyl hydroperoxide): OH reaction rate coefficients between 206 and 375 K and the OH photolysis quantum yield at 248 nm, Phys. Chem. Chem. Phys., 12, 12101–12111, doi:10.1039/C0CP00463D, 2010.

Berndt, T., Boge, O., and Stratmann, F.: Gas-phase ozonolysis of alpha-pinene: gaseous products and particle formation, Atmos. Environ., 37, 3933–3945, 2003.

Birdsall, A. W., Andreoni, J. F., and Elrod, M. J.: Investigation of the role of bicyclic peroxy radicals in the oxidation mechanism of toluene, J. Phys. Chem. A, 114, 10655–10663, 2010.

Blin-Simiand, N., Jorand, F., Sahetchian, K., Brun, M., Kerhoas, L., Malosse, C., and Einhorn, J.: Hydroperoxides with zero, one, two or more carbonyl groups formed during the oxidation of n-dodecane, Combust. Flame, 126, 1524–1532, doi:10.1016/s0010-2180(01)00264-4, 2001.

Capouet, M. and Müller, J.-F.: A group contribution method for estimating the vapour pressures of α-pinene oxidation products, Atmos. Chem. Phys., 6, 1455–1467, doi:10.5194/acp-6-1455-2006, 2006.

Capouet, M., Peeters, J., Noziere, B., and Müller, J.-F.: Alpha-pinene oxidation by OH: simulations of laboratory experiments, Atmos. Chem. Phys., 4, 2285–2311, doi:10.5194/acp-4-2285-2004, 2004.

Capouet, M., Mueller, J. F., Ceulemans, K., Compernolle, S., Vereecken, L., and Peeters, J.: Modeling aerosol formation in alpha-pinene photo-oxidation experiments, J. Geophys. Res.-Atmos., 113, D02308, doi:10.1029/2007JD008995, 2008.

Carter, W. P. L., Darnall, K. R., Graham, R. A., Winer, A. M., and Pitts, J. N.: Reactions of C_2 and C_4 alpha-hydroxy radicals with

oxygen, J. Phys. Chem., 83, 2305–2311, 1979.

Chung, S. H. and Seinfeld, J. H.: Global distribution and climate forcing of carbonaceous aerosols, J. Geophys. Res.-Atmos., 107, doi:10.1029/2001JD001397, 2002.

Cocker, D. R. I., Flagan, R. C., and Seinfeld, J. H.: State-of-the-art chamber facility for studying atmospheric aerosol chemistry, Environ. Sci. Technol., 35, 2594–2601, 2001.

Crounse, J. D., McKinney, K. A., Kwan, A. J., and Wennberg, P. O.: Measurement of gas-phase hydroperoxides by chemical ionization mass spectrometry, Anal. Chem., 78, 6726–6732, 2006.

Crounse, J. D., Paulot, F., Kjaergaard, H. G., and Wennberg, P. O.: Peroxy radical isomerization in the oxidation of isoprene, Phys. Chem. Chem. Phys., 13, 13607–13613, doi:10.1039/C1CP21330J, 2011.

da Silva, G., Graham, C., and Wang, Z.-F.: Unimolecular beta-Hydroxyperoxy Radical Decomposition with OH Recycling in the Photochemical Oxidation of Isoprene, Environ Sci. Technol., 44, 250–256, doi:10.1021/es900924d, 2010.

Davis, M. E., Talukdar, R. K., Notte, G., Ellison, G. B., and Burkholder, J. B.: Rate coefficients for the OH plus pinonaldehyde ($C_{10}H_{16}O_2$) reaction between 297 and 374 K, Environ. Sci. Technol., 41, 3959–3965, 2007.

Dillon, T. J. and Crowley, J. N.: Direct detection of OH formation in the reactions of HO_2 with $CH_3C(O)O_2$ and other substituted peroxy radicals, Atmos. Chem. Phys., 8, 4877–4889, doi:10.5194/acp-8-4877-2008, 2008.

Goldstein, A. H. and Galbally, I. E.: Known and unexplored organic constituents in the Earth's atmosphere, Environ. Sci. Technol., 41, 1514–1521, 2007.

Grosjean, D.: Atmospheric chemistry of alcohols, J. Braz. Chem. Soc., 8, 433–442, 1997.

Guenther, A., Hewitt, C. N., Erickson, D., Fall, R., Geron, C., Graedel, T., Harley, P., Klinger, L., Lerdau, M., Mckay, W. A., Pierce, T., Scholes, B., Steinbrecher, R., Tallamraju, R., Taylor, J., and Zimmerman, P.: A global model of natural volatile organic compound emissions, J. Geophys. Res.-Atmos., 100, 8873–8892, doi:10.1029/94JD02950, 1995.

Hasson, A. S., Tyndall, G. S., and Orlando, J. J.: A product yield study of the reaction of HO_2 radicals with ethyl peroxy ($C_2H_5O_2$), acetyl peroxy ($CH_3C(O)O_2$), and acetonyl peroxy ($CH_3C(O)CH_2O_2$) radicals, J. Phys. Chem. A, 108, 5979–5989, 2004.

Hatakeyama, S., Izumi, K., Fukuyama, T., Akimoto, H., and Washida, N.: Reactions of OH with alpha-pinene and beta-pinene in air – Estimate of global CO production from the atmospheric oxidation of terpenes, J. Geophys. Res.-Atmos., 96, 947–958, 1991.

Hoffmann, T., Odum, J. R., Bowman, F., Collins, D., Klockow, D., Flagan, R. C., and Seinfeld, J. H.: Formation of organic aerosols from the oxidation of biogenic hydrocarbons, J. Atmos. Chem., 26, 189–222, doi:10.1029/90JD02341, 1997.

Ianni, J. C.: Kintecus, Window v. 2.80, www.kintecus.com, 2002.

Jaoui, M. and Kamens, R. M.: Mass balance of gaseous and particulate products analysis from alpha-pinene/NO_x/air in the presence of natural sunlight, J. Geophys. Res.-Atmos., 106, 12541–12558, doi:10.1029/2001JD900005, 2001.

Jorand, F., Heiss, A., Perrin, O., Sahetchian, K., Kerhoas, L., and Einhorn, J.: Isomeric hexyl-ketohydroperoxides formed by reactions of hexoxy and hexylperoxy radicals in oxygen, Int. J. Chem.

Kinet., 35, 354–366, doi:10.1002/kin.10136, 2003.

Kavouras, I. G., Mihalopoulos, N., and Stephanou, E. G.: Formation of atmospheric particles from organic acids produced by forests, Nature (London), 395, 683–686, 1998.

Kavouras, I. G., Mihalopoulos, N., and Stephanou, E. G.: Formation and gas/particle partitioning of monoterpenes photooxidation products over forests, Geophys. Res. Lett., 26, 55–58, doi:10.1029/1998GL900251, 1999.

Keywood, M. D., Varutbangkul, V., Bahreini, R., Flagan, R. C., and Seinfeld, J. H.: Secondary organic aerosol formation from the ozonolysis of cycloalkenes and related compounds, Environ. Sci. Technol., 38, 4157–4164, 2004.

Kwok, E. S. C. and Atkinson, R.: Estimation of hydroxyl radical reaction rate constants for gas-phase organic compounds using a structure-reactivity relationship: an update, Atmos. Environ., 29, 1685–1695, 1995.

Laaksonen, A., Kulmala, M., O'Dowd, C. D., Joutsensaari, J., Vaattovaara, P., Mikkonen, S., Lehtinen, K. E. J., Sogacheva, L., Dal Maso, M., Aalto, P., Petäjä, T., Sogachev, A., Yoon, Y. J., Lihavainen, H., Nilsson, D., Facchini, M. C., Cavalli, F., Fuzzi, S., Hoffmann, T., Arnold, F., Hanke, M., Sellegri, K., Umann, B., Junkermann, W., Coe, H., Allan, J. D., Alfarra, M. R., Worsnop, D. R., Riekkola, M.-L., Hyötyläinen, T., and Viisanen, Y.: The role of VOC oxidation products in continental new particle formation, Atmos. Chem. Phys., 8, 2657–2665, doi:10.5194/acp-8-2657-2008, 2008.

Larsen, B. R., Di Bella, D., Glasius, M., Winterhalter, R., Jensen, N. R., and Hjorth, J.: Gas-phase OH oxidation of monoterpenes: Gaseous and particulate products, J. Atmos. Chem., 38, 231–276, 2001.

Lee, A., Goldstein, A. H., Kroll, J. H., Ng, N. L., Varutbangkul, V., Flagan, R. C., and Seinfeld, J. H.: Gas-phase products and secondary aerosol yields from the photooxidation of 16 different terpenes, J. Geophys. Res.-Atmos., 111, D17305, doi:10.1029/2006JD007050, 2006.

Lelieveld, J., Butler, T. M., Crowley, J. N., Dillon, T. J., Fischer, H., Ganzeveld, L., Harder, H., Lawrence, M. G., Martinez, M., Taraborrelli, D., and Williams, J.: Atmospheric oxidation capacity sustained by a tropical forest, Nature, 452, 737–740, 2008.

Librando, V. and Tringali, G.: Atmospheric fate of OH initiated oxidation of terpenes. Reaction mechanism of alpha-pinene degradation and secondary organic aerosol formation, J. Environ. Manage., 75, 275–282, 2005.

Monks, P. S., Granier, C., Fuzzi, S., Stohl, A., Williams, M. L., Akimoto, H., Amann, M., Baklanov, A., Baltensperger, U., Bey, I., Blake, N., Blake, R. S., Carslaw, K., Cooper, O. R., Dentener, F., Fowler, D., Fragkou, E., Frost, G. J., Generoso, S., Ginoux, P., Grewe, V., Guenther, A., Hansson, H. C., Henne, S., Hjorth, J., Hofzumahaus, A., Huntrieser, H., Isaksen, I. S. A., Jenkin, M. E., Kaiser, J., Kanakidou, M., Klimont, Z., Kulmala, M., Laj, P., Lawrence, M. G., Lee, J. D., Liousse, C., Maione, M., McFiggans, G., Metzger, A., Mieville, A., Moussiopoulos, N., Orlando, J. J., O'Dowd, C. D., Palmer, P. I., Parrish, D. D., Petzold, A., Platt, U., Pöschl, U., Prevot, A. S. H., Reeves, C. E., Reimann, S., Rudich, Y., Sellegri, K., Steinbrecher, R., Simpson, D., ten Brink, H., Theloke, J., van der Werf, G. R., Vautard, R., Vestreng, V., Vlachokostas, C., and von Glasow, R.: Atmospheric composition change – global and regional air quality, Atmos. Environ., 43, 5268–5350, 2009.

Müller, L., Reinnig, M.-C., Naumann, K. H., Saathoff, H., Mentel, T. F., Donahue, N. M., and Hoffmann, T.: Formation of 3-methyl-1,2,3-butanetricarboxylic acid via gas phase oxidation of pinonic acid – a mass spectrometric study of SOA aging, Atmos. Chem. Phys., 12, 1483–1496, doi:10.5194/acp-12-1483-2012, 2012.

Nguyen, T. L., Vereecken, L., and Peeters, J.: HO$_x$ Regeneration in the Oxidation of Isoprene III: Theoretical Study of the key Isomerisation of the Z-delta-hydroxy-peroxy Isoprene Radicals, Chem. Phys. Chem., 11, 3996–4001, doi:10.1002/cphc.201000480, 2010.

Niki, H., Maker, P. D., Savage, C. M., and Breitenbach, L. P.: A Fourier transform infrared study of the kinetics and mechanism for the reaction hydroxyl + methyl hydroperoxide, J. Phys. Chem., 87, 2190–2193, 1983.

Noell, A. C., Alconcel, L. S., Robichaud, D. J., Okumura, M., and Sander, S. P.: Near-Infrared kinetic spectroscopy of the HO$_2$ and C$_2$H$_5$O$_2$ self-reactions and cross reactions, J. Phys. Chem. A, 114, 6983–6995, 2010.

Noziere, B., Barnes, I., and Becker, K.-H.: Product study and mechanisms of the reactions of alpha -pinene and of pinonaldehyde with OH radicals, J. Geophys. Res.-Atmos., 104, 23645–23656, doi:10.1029/1999JD900778, 1999.

Paulot, F., Crounse, J. D., Kjaergaard, H. G., Kroll, J. H., Seinfeld, J. H., and Wennberg, P. O.: Isoprene photooxidation: new insights into the production of acids and organic nitrates, Atmos. Chem. Phys., 9, 1479–1501, doi:10.5194/acp-9-1479-2009, 2009a.

Paulot, F., Crounse, J. D., Kjaergaard, H. G., Kurten, A., St. Clair, J. M., Seinfeld, J. H., and Wennberg, P. O.: Unexpected epoxide formation in the gas-phase photooxidation of isoprene, Science, 325, 730–733, 2009b.

Peeters, J. and Muller, J. F.: HO$_x$ radical regeneration in isoprene oxidation via peroxy radical isomerisations. II: experimental evidence and global impact, Phys. Chem. Chem. Phys., 12, 14227–14235, doi:10.1039/C0CP00811G, 2010.

Peeters, J., Nguyen, T. L., and Vereecken, L.: HO$_x$ radical regeneration in the oxidation of isoprene, Phys. Chem. Chem. Phys., 11, 5935–5939, 2009.

Perrin, O., Heiss, A., Doumenc, F., and Sahetchian, K.: Homogeneous and heterogeneousreactions of the n-C$_5$H$_{11}$O, n-C$_5$H$_{10}$OH and OOC$_5$H$_{10}$OH radicals in oxygen. Analytical-steady state solution by use of the Laplace transform, J. Chem. Soc. Faraday T., 94, 2323–2335, doi:10.1039/a803340d, 1998.

Pye, H. O. T., Chan, A. W. H., Barkley, M. P., and Seinfeld, J. H.: Global modeling of organic aerosol: the importance of reactive nitrogen (NO$_x$ and NO$_3$), Atmos. Chem. Phys., 10, 11261–11276, doi:10.5194/acp-10-11261-2010, 2010.

Raventros-Duran,M. T., Percival, C. J., McGillen, M. R., Hamer, P. D., and Shallcross, D. E.: Kinetics and branching ratio studies of the reaction of C$_2$H$_5$O$_2$ + HO$_2$ using chemical ionization mass spectrometry, Phys. Chem. Chem. Phys., 9, 4338–4348, doi:10.1039/B703038J, 2007.

Ren, X., Olson, J. R., Crawford, J. H., Brune, W. H., Mao, J., Long, R. B., Chen, Z., Chen, G., Avery, M. A., Sachse, G. W., Barrick, J. D., Diskin, G. S., Huey, L. G., Fried, A., Cohen, R. C., Heikes, B., Wennberg, P. O., Singh, H. B., Blake, D. R., and Shetter, R. E.: HO$_x$ chemistry during INTEX-A 2004: observation, model calculation, and comparison with previous studies, J. Geophys. Res.-Atmos., 113, D05310, doi:10.1029/2007JD009166, 2008.

Sander, S. P., Finlayson-Pitts, B. J., Friedl, R. R., Golden, D. M., Huie, R. E., Kolb, C. E., Kurylo, M. J., Molina, M. J., Moortgat, G. K., Orkin, V. L., and Ravishankara, A. R.: Chemical kinetics and photochemical data for use in atmospheric studies, evaluation number 15, Tech. rep., Jet Propulsion Laboratory, 2006.

Saunders, S. M., Jenkin, M. E., Derwent, R. G., and Pilling, M. J.: Protocol for the development of the Master Chemical Mechanism, MCM v3 (Part A): tropospheric degradation of non-aromatic volatile organic compounds, Atmos. Chem. Phys., 3, 161–180, doi:10.5194/acp-3-161-2003, 2003.

St. Clair, J. M., McCabe, D. C., Crounse, J. D., Steiner, U., and Wennberg, P. O.: Chemical ionization tandem mass spectrometer for the in situ measurement of methyl hydrogen peroxide, Rev. Sci. Instrum., 81, 094102, doi:10.1063/1.3480552, 2010.

Steinbrecher, R., Smiatek, G., Koeble, R., Seufert, G., Theloke, J., Hauff, K., Ciccioli, P., Vautard, R., and Curci, G.: Intra- and inter-annual variability of VOC emissions from natural and semi-natural vegetation in Europe and neighbouring countries, Atmos. Environ., 43, 1380–1391, 2009.

Szmigielski, R., Surratt, J. D., Gomez-Gonzalez, Y., Van der Veken, P., Kourtchev, I., Vermeylen, R., Blockhuys, F., Jaoui, M., Kleindienst, T. E., Lewandowski, M., Offenberg, J. H., Edney, E. O., Seinfeld, J. H., Maenhaut, W., and Claeys, M.: 3-methyl-1,2,3-butanetricarboxylic acid: an atmospheric tracer for terpene secondary organic aerosol, Geophys. Res. Lett., 34, L24811, doi:10.1029/2007GL031338, 2007.

Taylor, W. D., Allston, T. D., Moscato, M. J., Fazekas, G. B., Kozlowski, R., and Takacs, G. A.: Atmospheric photo-dissociation lifetimes for nitromethane, methyl nitrite, and methyl nitrate, Int. J. Chem. Kinet., 12, 231–240, doi:10.1002/kin.550120404, 1980.

Vaghjiani, G. L. and Ravishankara, A. R.: Kinetics and mechanism of OH reaction with CH$_3$OOH, J. Phys. Chem., 93, 1948–1959, 1989.

Vereecken, L. and Peeters, J.: Enhanced H-atom abstraction from pinonaldehyde, pinonic acid, pinic acid, and related compounds: theoretical study of C-H bond strengths, Phys. Chem. Chem. Phys., 4, 467–472, doi:10.1039/B109370C, 2002.

Vereecken, L., Muller, J. F., and Peeters, J.: Low-volatility poly-oxygenates in the OH-initiated atmospheric oxidation of alpha-pinene: impact of non-traditional peroxyl radical chemistry, Phys. Chem. Chem. Phys., 9, 5241–5248, doi:10.1039/B708023A, 2007.

Wang, C. and Chen, Z.: An experimental study for rate constants of the gas phase reactions of CH$_3$CH$_2$OOH with OH radicals, O$_3$, NO$_2$ and NO, Atmos. Environ., 42, 6614–6619, 2008.

Wisthaler, A., Jensen, N. R., Winterhalter, R., Lindinger, W., and Hjorth, J.: Measurements of acetone and other gas phase product yields from the OH-initiated oxidation of terpenes by proton-transfer-reaction mass spectrometry (PTR-MS), Atmos. Environ., 35, 6181–6191, 2001.

Wolfe, G. M., Thornton, J. A., Bouvier-Brown, N. C., Goldstein, A. H., Park, J.-H., McKay, M., Matross, D. M., Mao, J., Brune, W. H., LaFranchi, B. W., Browne, E. C., Min, K.-E., Wooldridge, P. J., Cohen, R. C., Crounse, J. D., Faloona, I. C., Gilman, J. B., Kuster, W. C., de Gouw, J. A., Huisman, A., and Keutsch, F. N.: The Chemistry of Atmosphere-Forest Exchange (CAFE) Model – Part 2: Application to BEARPEX-2007 observations, Atmos. Chem. Phys., 11, 1269–1294, doi:10.5194/acp-11-1269-2011, 2011.

Yu, J., Griffin, R. J., Cocker, David R., I., Flagan, R. C., Seinfeld, J. H., and Blanchard, P.: Observation of gaseous and particulate products of monoterpene oxidation in forest atmospheres, Geophys. Res. Lett., 26, 1145–1148, doi:10.1029/1999GL900169, 1999.

Zhang, Y. Y., Müller, L., Winterhalter, R., Moortgat, G. K., Hoffmann, T., and Pöschl, U.: Seasonal cycle and temperature dependence of pinene oxidation products, dicarboxylic acids and nitrophenols in fine and coarse air particulate matter, Atmos. Chem. Phys., 10, 7859–7873, doi:10.5194/acp-10-7859-2010, 2010.